physica status solidi

pss

www.pss-journals.com

reprint

WILEY-VCH

Phys. Status Solidi B **252**, No. 8, 1868–1871 (2015) / **DOI** 10.1002/pssb.201552119

physica status solidi b
www.pss-b.com
basic solid state physics

Electron confinement in graphene with gate-defined quantum dots

Holger Fehske,*[,1] Georg Hager,[2] and Andreas Pieper[1]

[1] Institut für Physik, Ernst-Moritz-Arndt-Universität Greifswald, 17487 Greifswald, Germany
[2] Regionales Rechenzentrum Erlangen, Universität Erlangen-Nürnberg, 91058 Erlangen, Germany

Received 18 January 2015, revised 2 March 2015, accepted 2 March 2015
Published online 31 March 2015

Keywords electronic transport, graphene-based nanostructures, particle confinement, quantum dot arrays, scattering

* Corresponding author: e-mail fehske@physik.uni-greifswald.de, Phone: +49 3834 864760, Fax: +49 3834 864701

We theoretically analyse the possibility to electrostatically confine electrons in circular quantum dot arrays, impressed on contacted graphene nanoribbons by top gates. Utilising exact numerical techniques, we compute the scattering efficiency of a single dot and demonstrate that for small-sized scatterers the cross-sections are dominated by quantum effects, where resonant scattering leads to a series of quasi-bound dot states. Calculating the conductance and the local density of states for quantum dot superlattices, we show that the resonant carrier transport through such graphene-based nanostructures can be easily tuned by varying the gate voltage.

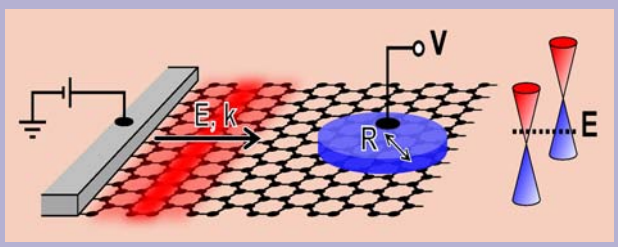

Schematic representation of a Dirac electron wave packet impinging on a circular, electrostatically defined quantum dot.

1 Introduction High-quality graphene nanostructures are the most likely building blocks in future electronics, plasmonics and photonics assemblies. Most of their striking features arise from the strictly two-dimensional, honeycomb lattice structure of the basic material, which causes the non-trivial topology of the electronic wave function and an almost linear low-energy spectrum of the chiral quasiparticles (charge carriers) near the so-called Dirac nodal points [1]. From an application-technological point of view, the tunability of the transport properties of graphene by external electric and magnetic fields is of particular importance [2]. This allows a controlled modification of selected areas of the sample by gating. For instance, applying nanoscale top gates on graphene nanoribbons (GNRs) or bilayer graphene, single or double quantum dots with particular shape have been produced in recent experiments [3–5].

For a large circular dot, the refraction at the boundary gives rise to two coalescing caustics that focus the electron density in the disk-shaped region [6, 7]. Resonances in the conductance [8] and the scattering cross section [9] indicate electron confinement for small quantum dots in monolayer graphene as well. Apparently the difficulty to localise Dirac electrons by electrostatic potential barriers (which is related to the Klein tunnelling phenomenon) could be overcome: Because of the circular symmetry, the angle of incidence at the dot's boundary is a constant of motion so that electrons with nonzero angular momentum are confined [8]. Forward scattering and Klein tunnelling will also be suppressed if a Fano resonance arises between the background partition and the resonant contribution to electron scattering [9]. These results, obtained within continuum Dirac theory, were numerically confirmed for a lattice model [10, 11]. The role of resonances have been analysed in various graphene scattering experiments [12, 13]. Note that the scattering (transport and optics) of massless Dirac fermions on potential barriers substantially differs from that of massive chiral Dirac fermions or Schrödinger electrons [14].

In this work, we address the scattering and (linear) transport in armchair GNRs with gate-defined quantum dots in the end-contacted lead-sample geometry most relevant for experiments [15–17]. The leads can be viewed as semi-infinite quantum wires; the contacts are metallic or gated graphene.

2 Model and numerical methods We describe the sample by the tight-binding Hamiltonian

$$H = \sum_i V_i c_i^\dagger c_i - t \sum_{\langle ij \rangle} (c_i^\dagger c_j + \text{H.c.}) \,, \tag{1}$$

where $c_i^{(\dagger)}$ annihilates (creates) an electron at Wannier site i of a honeycomb lattice with carbon–carbon distance $a = 1.42$ Å. Here, the hopping amplitude between nearest neighbour sites $\langle ij \rangle$ is given by t ($\simeq$3 eV) and the site-dependent potentials $V_i = V \sum_n \Theta(R - |\boldsymbol{r}_i - \boldsymbol{r}_n|)$ model electrostatically defined quantum dots with radius R centred at positions $\boldsymbol{r}_n$.

In the limit of vanishing bias voltage, the conductance between the left (L) and right (R) leads can be obtained within the limits of the Landauer–Büttiker approach:

$$G_{\text{LR}} = \frac{e^2}{h} \sum_{n \in \text{L}, m \in \text{R}} |S_{n,m}|^2 \,, \tag{2}$$

where $S_{n,m}$ is the scattering matrix between all open (i.e., active) lead channels [18]. We furthermore exploit the local density of states (LDOS) at a certain site i of the sample,

$$\text{LDOS}(E) = \sum_l |\langle i|l \rangle|^2 \delta(E - E_l) \,, \tag{3}$$

as a probe of a possible electrostatic confinement of the charge carrier [19, 20]. In Eq. (3), E is the particle's energy and the sum extends over all single-electron eigenstates $|l\rangle = c_l^\dagger |0\rangle$ of H with energy E_l. We use the kernel polynomial method [21] and the 'Kwant' software package [22] for evaluating the conductance and LDOS numerically.

3 Results and discussion

3.1 Single quantum dot First we consider a single dot, see Fig. 1. To begin with we determine the scattering efficiency Q, which is the scattering cross section divided by the geometric cross section, of a plane Dirac electron wave hitting on a dot embedded in an infinite graphene sheet, within the Dirac approximation (for details of such a calculation cf. Ref. [9]). Since the energy is conserved in our setup (i.e., there is no coupling to bath degrees of freedom, etc.), the scattering is always elastic (coherent). The data displayed in the upper panel for $E = 0.05\,t$ and $R = 5$ nm shows that a series of resonances appears when the gate voltage is varied (besides the rather broad a_0 and a_1 modes, the $a_{m>1}$ resonances are very sharp), which can be attributed to the excitations of higher dot normal modes [9]. So each maximum marks a combination of E, R and V, where a certain normal mode fits particularly well into the dot, while all other modes are suppressed. The middle panel indicates that these signatures also show up in the conductance, which this time, however, was computed for a 20 nm wide armchair GNR placed between leads. That is why we can assign the signal at $V \simeq -0.09\,t$ to the a_1 mode. The value for $G[V = 0]$ tells us that the system

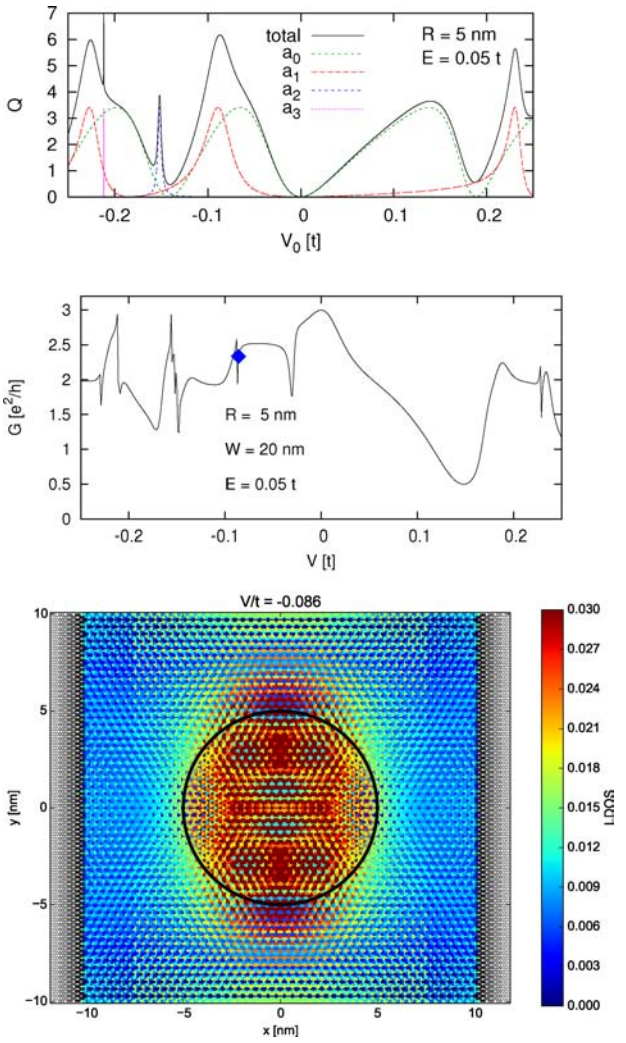

Figure 1 Total and partial scattering efficiencies (top), conductance (middle) and LDOS (bottom) of a single quantum dot (the black circle specifies the dimension of the dot). For further explanation see text.

exhibits three open transport channels. The lowermost panel presents the LDOS close to the a_1 resonance marked in the G versus V plot by the blue diamond. Obviously the electron is almost completely localised at the quantum dot, where the superposition of the states with $j = \pm(m + 1/2)$ leads to the characteristic vortex pattern of the a_1 mode. There are six vortices close to the boundary of the dot, which are reflected by three preferred scattering directions in the far field [9].

3.2 Quantum dot chain We now study quantum dots arranged like a string of pearls. Figure 2 presents the conductance and the LDOS for a contacted GNR sample with five dots at intervals of 20 nm. Again we set $R = 5$ nm, $E = 0.05t$, and the width of the armchair GNR is 20 nm. Note that the conductance undergoes a dramatic change if V is slightly varied near the resonance points (see red and blue diamonds). In this way, the system may act as a switch. The

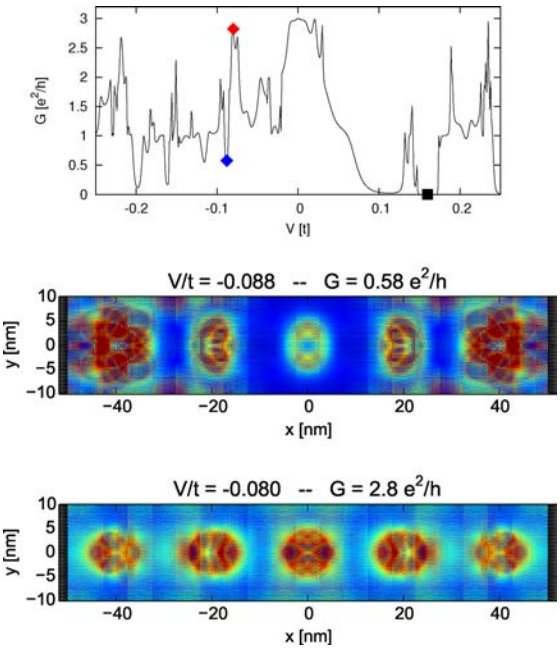

Figure 2 Conductance (top) and LDOS (lower panels) of a GNR with a linear array of quantum dots. The colour code is the same as in Fig. 1.

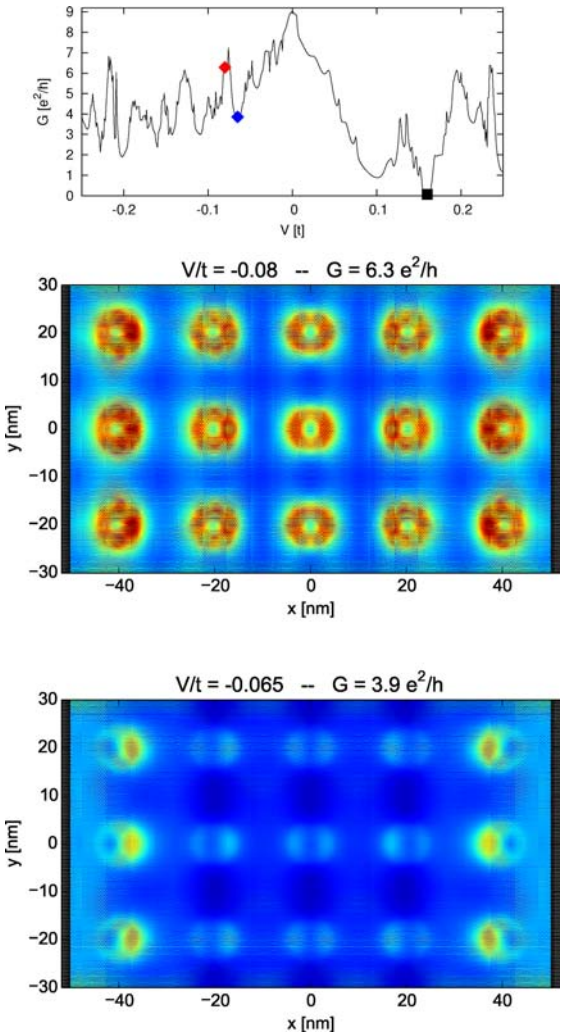

Figure 3 Conductance (top) and LDOS (middle/bottom) of an armchair GNR with a square dot superlattice.

results for the LDOS provide further insight into how the system behaves locally for $V = -0.088\,t$ ($V = -0.080\,t$), i.e., at the local minimum (maximum) of the conductance. At $V = -0.088\,t$, $E = 0.05t$ (middle panel), the quantum dots are off-resonance from an eigenmode of the particle: As a result the scattering is enhanced and the conductance is low (note that the figure shows a stationary situation). For an applied bias $V = -0.080\,t$ (lower panel) all dots largely support the a_1 mode. Since the wave functions of quasi-bound a_1 modes at neighbouring dots overlap resonantly, electrons are no longer permanently confined to a particular dot but will be transferred through the GNR by an effective inter-dot hopping process. Remarkably, in this case the conductance is almost as large as for the GNR without quantum dots ($G[V = 0]$) where the LDOS is the same (i.e., uniform) everywhere between the leads.

3.3 Quantum dot matrix Figure 3 illustrates that the same behaviour could be achieved for a square quantum dot superlattice made on an armchair GNR (now the width of the GNR is 60 nm, the other parameters are the same as in Fig. 2). For $V = 0$, the system has nine open transport channels. Again the relatively large conductance at $V = -0.080\,t$ (compared to G for $V = -0.065\,t$) originates from an effective (coherent) inter-dot transfer of the electron. This hopping process is expected to take place on a reduced time scale [11]. As can be seen from the lowermost panel, at $V = -0.065\,t$, the LDOS notably shrinks if we move to the centre of the GNR; this depletion of the local particle density reduces the inter-dot hopping and consequently the conductance.

While graphene has a gapless band structure and also the armchair GNRs considered in Figs. 1–3 have $G > 0$ for all E at $V = 0$ (i.e., there are always open transport channels), the conductance of the GNRs with imprinted quantum dots may tend to zero in certain ranges of V; see the black squares in Figs. 2 and 3. Apparently the linear and square lattice periodic arrays of gate-defined quantum dots give rise to new superlattice band structures, which exhibit energy (pseudo) gaps just as for ordinary solids [23]. This is reflected in the LDOS depicted in Fig. 4.

4 Conclusions To summarise, using exact numerics, we have studied the electronic and transport properties of contacted graphene nanoribbons with gate-defined quantum dots of realistic size (i.e., with a few thousand carbon atoms that feel the electrostatic potential step). The conductivity of such systems is very sensitive to the model parameters and can even vanish. This provides an opportunity to use them as switches by varying the top gate potential.

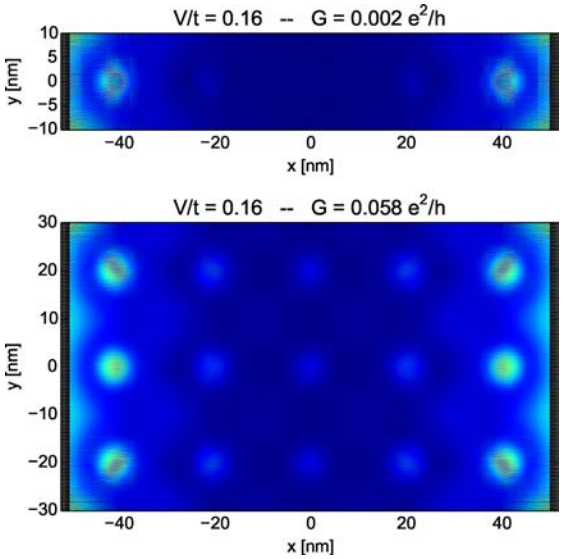

Figure 4 LDOS for a linear (top) and a square (bottom) quantum dot array on a GNR with almost vanishing conductance.

A detailed analysis of the local density of states shows that an electrostatic electron confinement is possible for single quantum dots in the quantum regime due to resonant scattering. Thereby the incident electron is fed into vortices, which trap the particle. That means for small dots the particle confinement is not by total internal reflection. In addition, for periodic quantum dot arrays a superlattice band structure evolves that allows for an effective inter-dot transport on a reduced energy scale. The phenomena detected in this work might be exploited in actual graphene-based devices. From a theoretical point of view, it seems worthwhile to study a modulation of the quantum dot barriers – via the top gates – by oscillating fields, which induces both inelastic tunnelling and resonant transport through excited states [24]. Another issue is the electrical and magneto transport through quantum dots on folded graphene samples that exhibit superlattice structures in itself [25]. We finally like to emphasise that such graphene quantum dots might used to construct logic gates and 'quantum computing' devices [26], which would be also an interesting topic for future studies.

Acknowledgements This work was funded by the Deutsche Forschungsgemeinschaft through Priority Program SPP1459 'Graphene' and the Competence Network for Scientific High-Performance Computing in Bavaria (KONWIHR III, project PVSC-TM).

References

[1] A. H. Castro Neto, F. Guinea, N. M. R. Peres, K. S. Novoselov, and A. K. Geim, Rev. Mod. Phys. **81**, 109–162 (2009).
[2] M. O. Goerbig, Rev. Mod. Phys. **83**, 1193 (2011).
[3] X. L. Liu, D. Hug, and L. M. K. Vandersypen, Nano Lett. **10**, 1623 (2010).
[4] M. T. Allen, J. Martin, and A. Yacoby, Nature Commun. **8**, 934 (2012).
[5] A. Müller, B. Kaestner, F. Hohls, T. Weimann, K. Pierz, and H. W. Schumacher, J. Appl. Phys. **115**, 233710 (2014).
[6] J. Cserti, A. Pályi, and C. Péterfalvi, Phys. Rev. Lett. **99**, 246801 (2007).
[7] M. M. Asmar and S. E. Ulloa, Phys. Rev. B **87**, 075420 (2013).
[8] J. H. Bardarson, M. Titov, and P. W. Brouwer, Phys. Rev. Lett. **102**, 226803 (2009).
[9] R. L. Heinisch, F. X. Bronold, and H. Fehske, Phys. Rev. B **87**, 155409 (2013).
[10] G. Pal, W. Apel, and L. Schweitzer, Phys. Rev. B **84**, 075446 (2011).
[11] A. Pieper, R. Heinisch, and H. Fehske, Europhys. Lett. **104**, 47010 (2013).
[12] X. Hong, K. Zou, and J. Zhu, Phys. Rev. B **80**, 241415 (2009).
[13] M. Monteverde, C. Ojeda-Aristizabal, R. Weil, K. Bennaceur, M. Ferrier, S. Guéron, C. Glattli, H. Bouchiat, J. N. Fuchs, and D. L. Maslov, Phys. Rev. Lett. **104**, 126801 (2010).
[14] P. E. Allain and J. N. Fuchs, Eur. Phys. J. B **83**, 301 (2011).
[15] S. Krompiewski, Nanotechnology **23**, 135203 (2012).
[16] L. Rosales and J. W. Gonzáles, Nanoscale Res. Lett. **8**, 5742 (2013).
[17] T. Lehmann, D. A. Ryndyk, and G. Cuniberti, Phys. Rev. B **88**, 125420 (2013).
[18] S. Datta, Electronic Transport in Mesoscopic Systems (Cambridge University Press, Cambridge, 1995).
[19] A. Pieper, R. L. Heinisch, G. Wellein, and H. Fehske, Phys. Rev. B **89**, 165121 (2014).
[20] M. Schneider and P. W. Brouwer, Phys. Rev. B **89**, 205437 (2014).
[21] A. Weiße, G. Wellein, A. Alvermann, and H. Fehske, Rev. Mod. Phys. **78**, 275 (2006).
[22] C. W. Groth, M. Wimmer, A. R. Akhmerov, and X. Waintal, New J. Phys. **16**(6), 063065 (2014).
[23] W. Liu, Z. F. Wang, Q. W. Shi, J. Yang, and F. Liu, Phys. Rev. B **80**, 233405 (2013).
[24] C. Schulz, R. L. Heinisch, and H. Fehske, Phys. Rev. B **91**, 045130 (2015).
[25] H. Schmidt, J. C. Rode, D. Smirnov, and R. J. Haug, Nature Commun. **5**, 5742 (2014).
[26] Z. F. Wang and F. Lui, Nanoscale **3**, 4201 (2011).